Direct measurement of darkness using a standard single-photon avalanche photodiode

Reep, T.H.A. van der; Molenaar, D.; Löffler, W.

Journal of the Optical Society of America A
OPTICS, IMAGE SCIENCE, AND VISION

Direct measurement of darkness using a standard single-photon avalanche photodiode

T. H. A. VAN DER REEP,[1,*] D. MOLENAAR,[2] AND W. LÖFFLER[1]

[1]Leiden Institute of Physics, Niels Bohrweg 2, 2333 CA Leiden, The Netherlands
[2]Psychology Research Institute, Nieuwe Achtergracht 129b, 1018 WS Amsterdam, The Netherlands
*reep@physics.leidenuniv.nl

Received 14 November 2024; revised 7 February 2025; accepted 17 February 2025; posted 19 February 2025; published 27 March 2025

In experiments requiring extreme darkness, such as experiments probing the limits of human vision, assessment of the background photon flux is essential. However, direct measurement thereof with standard single-photon detectors is challenged by dark counts and their fluctuations. Here we report an experiment and detailed statistical analysis of a direct measurement of darkness in a dedicated dark chamber suitable for human vision experiments, only using a standard single-photon detector and a mechanical shutter. From a Bayesian analysis of 616 h of data, we find substantial to decisive evidence for absolute darkness (depending on the choice of prior distribution) based on the Savage–Dickey ratio and a light level <0.039 cnt/s (posterior 0.95 highest density interval).

https://doi.org/10.1364/JOSAA.547686

1. INTRODUCTION

In psychophysics, the study of human perception, one of the parameters of interest is the smallest signal creating conscious perception. For the human visual system, it has been shown that photopic (color) vision mediated by cone photoreceptor cells is sensitive to photon states with order of 100 photons [1]. On the other hand, scotopic (low-light) vision using rod cells has been shown to be sensitive to few-photon states [2–4] using sources of Poissonian light. By using a source of spontaneous down-converted (SPDC) light, it was found that humans might even perceive single photons [5]. Given the noisy environment of the brain, and the low efficiency of the eye, this is quite remarkable. To increase our understanding of human vision in the few-photon limit further, we have recently proposed to study the perception of one- and few-photon states using quantum detector tomography [6].

In such studies, a dark chamber is of utmost importance. A common approach is to construct a dark chamber within a dark lab to null the background light that would add to experimental noise, which, apart from arising from a possible background, mainly originates from spontaneous activation of the photoreceptors. In rod cells, e.g., the number of dark activations is $(3.4 \pm 0.8) \times 10^{-3}\ \mathrm{s}^{-1}$ [7], implying approximately 50 dark activations per second if the experiment is performed using a Maxwellian view (light pulses focused on the eye lens [8]), in which the light pulses are directed to the area of the retina where the rod cell density is highest (1.6×10^5 rods/mm^2 [9]) with a half-opening angle of 0.4° and assuming a lens–retina distance of 24 mm. These dark activations directly compete with the weak few-photon signals to be perceived, and this task becomes even harder if any background light is present. However, to the best of our knowledge, measurements of the actual level of darkness during these experiments and other studies on human visual perception at low light-level [10–13] are typically not reported.

Assessment of darkness to levels below 0.1 photons/s/mm^2 is not easy due to dark counts in detection systems. For instance, standard single-photon detectors show 10–1000 dark counts per second. Therefore, one might attempt to measure the level of darkness of the lab environment, measure the attenuation of the dark chamber using a bright light source, and take the darkness level as the quotient of those values. Although this gives an estimate of how dark the dark chamber is, some important interpretation difficulties arise, especially when the goal is to measure absolute darkness. First, since the light source used in this "environment-attenuation" (EA) approach is spatially and spectrally different from the actual light sources that give rise to background light in the environment, one only *estimates* the attenuation of the dark chamber. Second, and more importantly, this method does not take into account the light generated *inside* the dark chamber, e.g., due to fluorescence, phosphorescence, or even low levels of radioactivity in the chambers' walls.

These issues can be overcome by using a *direct* measurement of the level of darkness, without using additional sources of light and from within the dark chamber itself. To this end, we place a single-photon detector in our dark chamber and connect it to a shutter. As such, we can study differences in the detector's

count distribution, dependent on whether the shutter is open or closed. In Section 2, we elaborate on the general method and describe the experimental setup of the dark lab and dark chamber, and in Section 3, the method is applied to assess the level of darkness in our dark chamber. We analyze the data using a Bayesian approach, which, contrary to frequentist approaches based on p-values [14], can be used to quantify both the presence and absence of evidence supporting the null hypothesis of absolute darkness. Our results from using the the EA approach are presented in Section 4, after which we provide a general discussion and conclusion in Sections 5 and 6, respectively.

2. METHOD

In order to test for absolute darkness, we use the following method. First, we darken the lab by applying sheets of 5 mm thick black foam board (Budget foamboard 5 mm 70 × 100 zwart) to all lab windows, which we fixate to each other and the window frame with 50 µm thick aluminum tape. A layer of black neoprene (Celrubberplaat EPDM zk 2 mm) with a thickness of 2 mm is applied as a weatherstrip to the inside of the lab door frame, thus preventing light from leaking in from the left, right, and top side of the door. The gap between the lower side of the door and the floor is covered with neoprene and a draught excluder. For the other doors in the lab, the gap between the door frame and door is closed with aluminum tape, whereas the lower gap is covered by neoprene. Other light leaks are covered by aluminum tape upon inspection.

Within the darkened lab, we additionally place two chambers (inverted grow tents [Phantom 90 × 150 × 200 cm ($W \times L \times H$)]). The white outer side of the chambers reflects impinging light, whereas the black inner side absorbs photons that have entered or are created in the chambers. The first chamber, the control chamber, contains the apparatuses controlling the experiment and prevents light produced by these devices from entering the lab. The latter chamber is our dark chamber. Both chambers are connected to a ventilation system to provide fresh air. Using a bended black hose, we prevent light from leaking from the control chamber into the dark chamber. A schematic overview of the lab is presented in Fig. 1(a), and some photographic details can be found in Supplement 1, Section S1.

To measure light levels in the dark chamber and lab, we use a single-photon counting module (SPCM, PerkinElmer SPCM-AQRH-14). This SPCM is located on a desk table in the dark chamber and detects single photons ($\lambda \approx 400-1060$ nm) using a silicon avalanche photodiode with a 180 µm diameter circular active area. The detector has a (time-varying) dark count rate of approximately $R_d = 200\ s^{-1}$. The SPCM is connected to a shutter (Uniblitz VS14 with D122 shutter driver) positioned approximately 35 mm in front of the photodiode using an in-house built adapter. With a shutter diameter of 14 mm, this implies the effective SPCM half-opening angle equals $\arctan(0.5 \cdot 14/35) = 11.3°$. One side of the shutter is black, whereas the other has a metallic finish, and we mount it such that the black side faces the SPCM. This setup allows to measure counts while the shutter is open (C_O, measuring dark counts plus light-counts) or closed (C_C, measuring dark counts only). The counts from the detector are collected and the shutter is controlled from a data acquisition (DAQ) card (National Instruments NI-6341) connected to a computer in the control chamber.

In this work we are concerned with measuring differences in C_O and C_C, which we evaluate using the difference distribution $\Delta \sim C_O - C_C$. To this end, we count the SPCM's TTL pulses during 1 s intervals in consecutive blocks of 10 s in which the shutter is open or closed using the internal 80 MHz clock of the DAQ card for timing. Hence, we measure for 10 1 s intervals with the shutter open, 10 intervals with the shutter closed, 10 intervals open, etc.; see Fig. 1(b). The shutter opens/closes during the first interval of the respective open/close blocks. These intervals are discarded for further analysis, in order to prevent the shutter motion from influencing C_O and C_C in any manner. By alternating the open/close blocks, the effect of time variations in dark count rate R_d can be mitigated. The difference distribution Δ is obtained by subtracting the number of counts in the i^{th} interval of C_O and C_C. Although these intervals are 10 s apart in time, R_d is not expected to vary within such a short time frame.

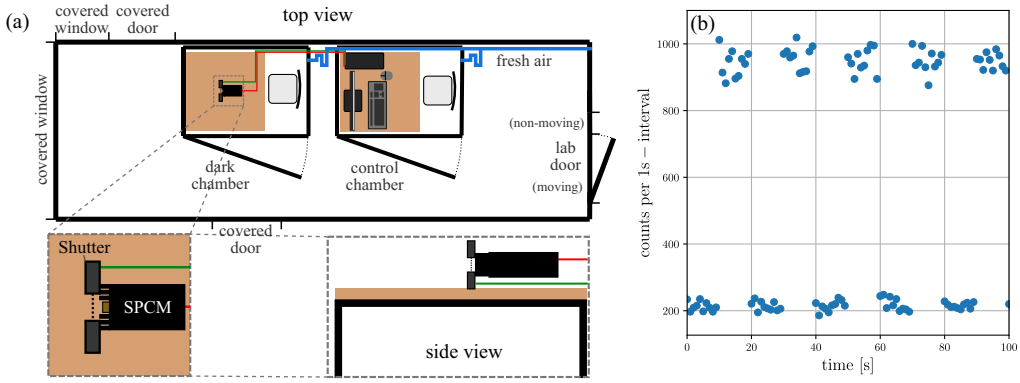

Fig. 1. Schematic overview of setup and method. (a) A dark lab is created by covering all lab windows and doors using sheets of black foam board, aluminum tape, and neoprene. Within the lab, two chambers are placed, one control chamber and the dark chamber. A shuttered SPCM is located inside the dark chamber to assess the level of darkness. (b) Opening and closing the shutter enables us to measure the difference in counts on the SPCM between the two shutter states. This is an example of data for a light level of approximately 750 cnt/s to illustrate the method. Count fluctuations are due to detector shot noise.

3. BAYESIAN ASSESSMENT OF DARKNESS

To perform a Bayesian assessment of darkness, we have written an analysis program in R [15]. We follow a Bayesian approach using RStan [16], fitting Δ measured within the dark chamber with a normal likelihood $\Delta \sim \mathcal{N}(\mu_\Delta, \sigma_\Delta^2)$. Thus, estimates are obtained for the unknown mean μ_Δ and standard deviation σ_Δ of Δ using Markov-Chain Monte Carlo (MCMC) sampling. As such, we sample from the posterior distributions of these parameters

$$p(\mu_\Delta, \sigma_\Delta|\Delta) \propto p(\Delta|\mu_\Delta, \sigma_\Delta)p(\mu_\Delta, \sigma_\Delta). \tag{1}$$

Here, $p(\Delta|\mu_\Delta, \sigma_\Delta)$ is the likelihood of the data and $p(\mu_\Delta, \sigma_\Delta)$ is the prior distribution for μ_Δ and σ_Δ, which we will denote as $p(\mu_\Delta^{(0)}, \sigma_\Delta^{(0)})$ from now on. Consequently, we will use the shorthand notation $p(\mu_\Delta^{(1)}, \sigma_\Delta^{(1)})$ for the posterior distribution. μ_Δ and σ_Δ^2 are the assigned the priors

$$\begin{aligned} \mu_\Delta^{(0)} &\sim \mathcal{N}(\mu_0, \sigma_0^2) \\ (\sigma_\Delta^2)^{(0)} &\sim \Gamma(\alpha_0, \beta_0). \end{aligned} \tag{2}$$

In which the prior mean μ_0 and variance σ_0^2 of the normal prior, and the shape parameters α_0 and β_0 of the gamma prior follow from the data:

$$\begin{aligned} \mu_0 &= \max(0, \text{mean}(\Delta)) & \beta_0 &= \frac{\text{var}(\Delta)\text{N}(\Delta)}{2f_\sigma \text{var}(\Delta)^2} = \frac{\text{N}(\Delta)}{2f_\sigma \text{var}(\Delta)} \\ \sigma_0^2 &= \frac{f_\mu \text{var}(\Delta)}{\text{N}(\Delta)} & \alpha_0 &= \text{var}(\Delta)\beta_0. \end{aligned} \tag{3}$$

In these equations, the variance of the mean [for σ_0^2, $\text{var}(\cdot)/\text{N}(\cdot)$, where $\text{N}(\cdot)$ refers to the total number of measurements performed] and the variance on the variance [for β_0, $2\text{var}(\cdot)^2/\text{N}(\cdot)$ [17]] of the normal distribution can be recognized. Both these variances are multiplied by factor, f_μ and f_σ, respectively, to broaden the prior distributions with respect to their expected distributions. As such, the priors become less informed. The choice of data-dependent prior parameters was made to make the analysis program also applicable in situations in which we do expect to measure an unknown amount of light-counts. In such a case, it seems a reasonable choice to add minimal information to the prior distributions in the form of an expected value, and to decrease the impact of this information by introducing prior broadening, thereby directly allowing for a sensitivity analysis. It should be noted that in the following we choose the prior broadening factors equal, $f_\mu = f_\sigma = f$, and that for our data $\mu_0 = 0$ (see below).

We assess the darkness in our dark chamber based on 616 h of measurements. This yields $0.9 \cdot 1800 \cdot 616 = 997920$ 1 s intervals sampling the distribution Δ. The measurements are summarized in Fig. 2. Here, in Fig. 2(a), it is observed that the distributions C_O and C_C shift over time as a result of fluctuations in R_d. As a result, these distributions are not directly comparable to assess the level of darkness in the dark chamber. This issue is no longer observed for Δ, for which mean and standard deviation have become constant in time; see Fig. 2(b). The measured distribution Δ is depicted in Fig. 2(c). The measured point mass function (PMF) is overlain with a PMF drawn from Gaussian distribution with the same mean (-4.14×10^{-3} cnt/s) and standard deviation (21.1 cnt/s), showing excellent agreement.

In our analysis of the data, we focus on the parameter $\mu_\Delta^{(1)}$ and quantify evidence for $\mu_\Delta^{(1)} = 0$ and $\mu_\Delta^{(1)} \neq 0$. The analysis results for $\mu_\Delta^{(1)}$ are shown in Fig. 3. In Fig. 3(a), the prior and posterior distribution for μ_Δ are depicted for a prior broadening factor of $f = 10$. These density plots are based on 6×10^4 MCMC samples drawn from $p(\mu_\Delta^{(1)})$ in RStan. The inset of this figure features the positive part of the distributions, corresponding to the requirement that the number of photons still present in the dark chamber must be strictly positive. From the full distribution, we obtain the probability of positive direction (adapted from the probability of direction [18] for purely positive effects), $\text{pd}^+ = p(\mu_\Delta^{(1)} > 0)$, as an indication of whether light has been detected ($\text{pd}^+ > 0.5$), and the Savage–Dickey (SD) ratio [19] as a Bayes' factor for absolute darkness. This ratio is given by $r_\text{SD}(0) = p(\mu_\Delta^{(1)} = 0)/p(\mu_\Delta^{(0)} = 0)$, where $p(\mu_\Delta^{(1)} = 0)$ is obtained from a logspline-fit of the MCMC samples' density using the logspline library available for R [20]. $p(\mu_\Delta^{(0)} = 0)$, on

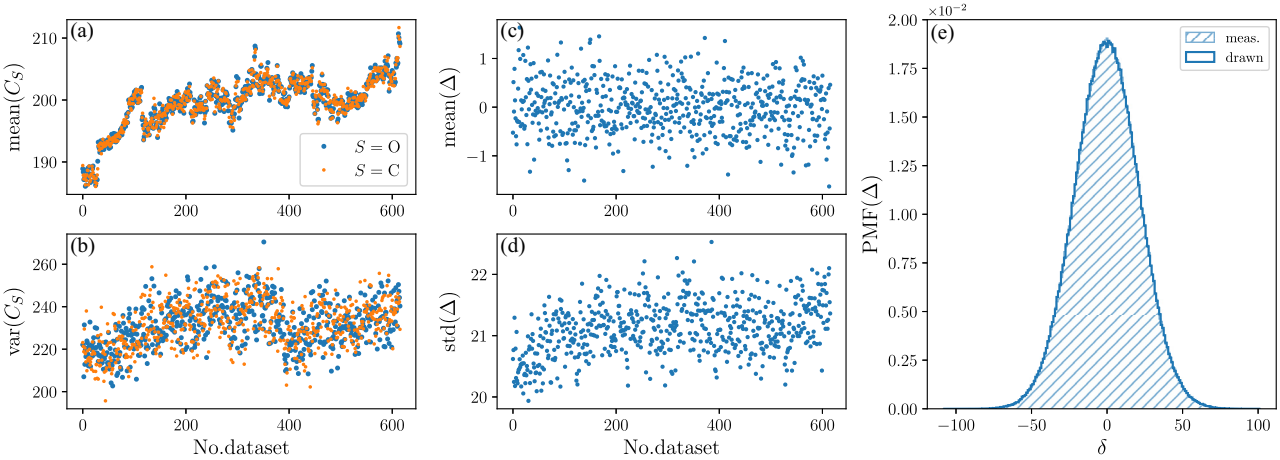

Fig. 2. Measured results for distributions C_O, C_C, and Δ after 616 h of measurement. (a) and (b) Mean and variance of distributions C_O and C_C per 1 h dataset. These values vary as a result of fluctuations in R_d. (c) and (d) Mean and standard deviation of Δ per 1 h dataset. These values are found to be constant. (e) Distribution of Δ. The hatched measured PMF is overlain with a PMF of samples drawn from a normal distribution with the same mean and standard deviation as the data.

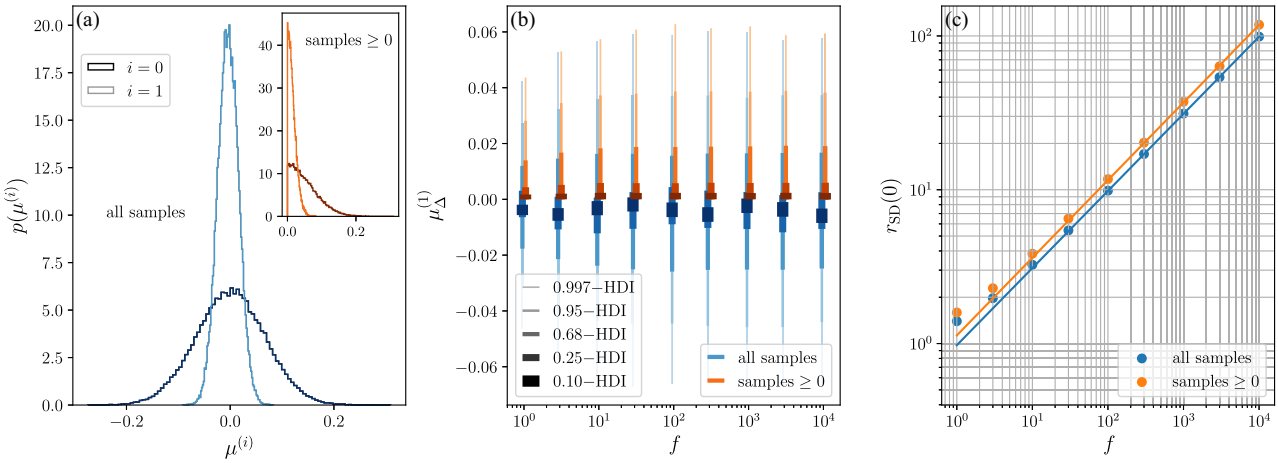

Fig. 3. RStan fit results for μ_Δ. (a) Prior and posterior distribution for $f = 10$. These distributions are analyzed in terms of the probability of positive direction, HDIs, and Savage–Dickey ratios. The inset shows the positive part of the distributions, stemming from the requirement that the number of photons still present must be strictly positive. (b) Posterior distribution as a function of f visualized using the indicated HDIs. For $f \geq 10$, the posterior is constant, indicating $f = 10$ is the minimum value for obtaining a posterior independent of the prior. (c) Savage–Dickey ratio for the null result (no light present) as function of f. Data points for $f \geq 10$ are fitted using a power function.

the other hand, follows directly from the prior distribution. We perform two hypothesis tests using the SD ratio:

- H_0:$\mu_\Delta = 0$ versus H_1:$\mu_\Delta \neq 0$ (using full distributions—evidence for μ_Δ not different from 0, given μ_Δ can be positive or negative), and
- H_0:$\mu_\Delta = 0$ versus H_1:$\mu_\Delta \geq 0$ (using positive part of distributions—evidence for μ_Δ not different from 0, given μ_Δ is strictly positive).

Finally, from the positive part of the distribution, highest density intervals (HDIs) are obtained as an upper limit to the light-counts detected.

In Figs. 3(b) and 3(c), the results of these measures can be observed for fits with different prior broadening factors f. Figure 3(b) depicts the posterior distribution for μ_Δ using the indicated HDIs for both the full distributions as well as its positive part. As can be seen, the distributions become constant for $f \geq 10$, indicating that for lower f, the fit is influenced by the choice of prior, which leads to an underestimation of HDIs. Therefore, we will not consider these fits in the following. From the full distribution, we find $\mu_\Delta^{(1)} = (-4.19 \pm 21.0) \times 10^{-3}$ cnt/s (mean $\pm$ standard deviation, 0.95 HDI $[-4.50, 3.71] \times 10^{-2}$ cnt/s), and we obtain a pd^+ of 0.42, indicating uncertainty in the direction of $\mu_\Delta^{(1)}$ [18]. Taking the 0.95 HDI as an upper limit to the number of light-counts detected, the positive part of the posterior yields the number of light-counts <0.039 cnt/s. On the other hand, as observed in Fig. 3(c), the SD ratio depends on f by a sqrt-dependence, as follows from a fit of the form $r_{SD}(0) = a\, f^b$. Based on these results, the evidence for absolute darkness is substantial ($r_{SD}(0) > 10^{1/2}$), strong ($r_{SD}(0) > 10^1$), very strong ($r_{SD}(0) > 10^{3/2}$), or even decisive ($r_{SD}(0) > 10^2$) [21], depending on the choice of f.

To assess the robustness of our results, we performed an alternative analysis using a Cauchy prior as proposed by, e.g., Refs. [21]–[23]. The advantage of such a prior is that the Bayes' factor can be calculated analytically. We use a location parameter of 0 and a scale parameter of 0.707, which is the default prior in the popular Bayesian analysis software package JASP [24]. This choice is comparable to setting $f = 0.707\mathrm{N}(\Delta) = 705529$ in our own analysis program. Results indicate that the Bayes' factor supporting the hypothesis that $\mu_\Delta = 0$ (given $\mu_\Delta \geq 0$) equals 1029.59, which is in agreement with $r_{SD}(0) \approx 1011$ given by our analysis. This indicates that there is decisive evidence in the data supporting the hypothesis that $\mu_\Delta = 0$.

4. ENVIRONMENT-ATTENUATION APPROACH

Additionally, we assess the level of darkness in our dark chamber using the EA approach. In this approach we measure the light level in the lab, $\bar{\Delta}_{\mathrm{lab}}$, as well as the attenuation of the dark chamber, A_c, using a bright light source. As such, an estimate of the light level in the dark chamber can be obtained as $\bar{\Delta}_{\mathrm{EA}} \approx \bar{\Delta}_{\mathrm{lab}}/A_c$.

For our EA measurements, the SPCM is rotated by 90° with respect to Fig. 1(a), such that it can detect light coming from the lab. In this position, the darkness level of the lab is assessed, while the dark chamber is open and found to be $\bar{\Delta}_{\mathrm{lab}} = 1.82 \pm 0.03$ cnt/s during 246 h of measurements (398520 samples).

Second, we estimate A_c. To this end, a bright 530 nm light-emitting diode (LED, Lumileds LXZ1-PM01) is mounted outside of the (still open) dark chamber, pointing toward the SPCM. At a current of 800 mA, the light level of this LED was measured to be $10^{9.10 \pm 0.01}$ cnt/s, as detailed in Supplement 1, Section S2. Thereafter, the light level of the bright LED on the SPCM is measured while the dark chamber is closed. This level was found to be 0.47 ± 0.09 cnt/s, based on 36 h of measurement (58320 samples). As such, we find that $A_c \approx 10^{9.10 \pm 0.01}/(0.47 \pm 0.09) = (2.8 \pm 0.6) \times 10^9$.

From $\bar{\Delta}_{\text{lab}}$ and A_c, we expect the light level in the dark chamber to be $\Delta_{\text{EA}} \approx 1.82 \pm 0.03/[(2.8 \pm 0.6) \times 10^9] = (6.9 \pm 1.8) \times 10^{-10}$ cnt/s.

5. DISCUSSION

The EA approach gives an estimate of the level of darkness orders of magnitude lower than the direct method [$(6.9 \pm 1.8) \times 10^{-10}$ cnt/s (EA) versus <0.039 cnt/s (direct)]. This discrepancy is inherent to the methods: in the EA approach, a (low) light level in the lab is divided by the (large) attenuation of the dark chamber, whereas the direct method relies on reducing the standard deviation on μ_Δ. However, as mentioned before, difficulties in interpretation arise for the former method, most importantly because it is insensitive to light generated inside the dark chamber itself. To clarify: we measured a darkness level of 0.47 ± 0.09 cnt/s in the closed dark chamber while the bright LED outside the chamber was switched on (see Section 4). However, within the EA approach, one cannot know whether *all* detected light originates from the bright LED. The light might as well be (partly) emitted from within the chamber itself by, e.g., phosphorescence. This problem of interpretation is circumvented by the direct method.

Yet, a similar argument can be made for the direct method. As shown in Supplement 1, Section S3, we infer a likely negative value of $\mu_\Delta^{(1)} = (-4.48 \pm 2.31) \times 10^{-2}$ cnt/s (0.95 HDI $[-9.0 \times 10^{-2},\ 6.0 \times 10^{-4}]$ cnt/s) in case the other (metallic-finished) side of the shutter faces the detector. We attribute this result to the reflection of SPCM-emitted flash photons from the shutter. This implies that the results shown in Section 3 might be offset by an unknown amount, e.g., if the detector would measure 10.000 cnt/s when the shutter is open due to background light in the dark chamber, and it would detect 10.004 cnt/s while the shutter is closed as a result of flash photons, we would obtain the same result. In Supplement 1, Section S4, we provide a simple model taking the contribution of reflected flash photons into account and find that the mentioned offset is absent if the black side of the shutter faces the detector.

It should be noted that the Bayesian approach is a slow method. After hundreds of hours of measurement, the upper limit on the light-clicks detected is still in the order of 10^{-2}. This is a direct result of the variance in the rate of dark counts produced in the SPCM in combination with the $\sqrt{N}$-law governing the width of the posterior distribution for μ_Δ. In absolute darkness, the 0.95 HDI length for the upper limit of the level of darkness will be given by

$$L_{0.95}^{\text{dark}} = 1.96\sqrt{\frac{2\text{var}(R_d)}{\text{N}(\Delta)}}, \tag{4}$$

where the factor 1.96 is the Gaussian z-score for the 0.95 HDI, and the variance in dark count rate is multiplied by 2, because we are subtracting two distributions to obtain Δ, C_C from C_O. From this equation, it is evident that using a detector with smaller var(R_d), such as a superconducting nanowire single-photon detector (SNSPD) [25], is more beneficial for reaching a lower upper limit for the number of light-counts. For such detectors, dark count rates of 10^{-4}s^{-1} have been reported. Assuming R_d of these detectors to be of the same order, our result could be reproduced with only 0.5 s of measurement time. The disadvantage of SNSPDs, however, is their operation at cryogenic temperatures, which greatly increases the experimental complexity. Still, it should be noted that even with such devices, an upper limit of zero will never be achieved. Alternatively, single-photon sensitive cameras, such as an electron-multiplying charge-coupled device (EMCCD) [26], could be utilized to study positional variation in background light, such that remaining light sources can be discovered and mitigated. This method also comes with the cost of increased experimental complexity, however.

Still, since the probability of positive direction $\text{pd}^+ = 0.42$ is uncertain as to which direction $p(\mu_\Delta^{(1)})$ favors, and $r_{\text{SD}}(0)$ yields substantial to decisive evidence for $\mu_\Delta^{(1)} = 0$, our results suggest the dark chamber to be absolutely dark. Note that $r_{\text{SD}}(\mu_\delta)$ would also give evidence for $\mu_\delta > 0$, but for our data, the result clearly peaks for $\mu_\delta = 0$; see Fig. 3(a). The amount of evidence for absolute darkness depends critically on the prior broadening factors f_μ and f_σ. In analyzing the data of this and similar experiments, the choice for these factors could be based on prior knowledge, e.g., from previous experiments. If such knowledge is absent (as in the present study), we recommend using $f = 0.707\text{N}(\Delta)$, so that the resulting (uninformative) prior is comparable to the default prior in JASP. However, it is recommendable to conduct a sensitivity analysis, similar to our analysis in Fig. 3(c), in order to study the robustness of the result.

In terms of the human eye, these results can be understood as follows. The shutter diameter and position with respect to the SPCM photodiode are such that the half-opening angle is approximately equal to the half-opening angle of the retina due to the pupil (a pupil diameter equal to 10 mm and pupil–retina distance of 24 mm yields a half-opening angle of 11.7°, only slightly larger than the 11.3° for the SPCM). Neglecting the quantum efficiency of the SPCM, the loss in the vitreous body, and the sensitivity of the retina's rods and cones, our results compare directly to the number of 400–1060 nm background photons reaching an area of $\pi \cdot (180\ \mu\text{m}/2)^2$ of the retina. Hence, if during actual psychophysical experiments, light pulses reach the retina within a circular area of diameter d, the upper limit to the number of counts caused by background light within this area is $0.039 \cdot d/(180\ \mu\text{m})\text{s}^{-1}$. Thus, if the light pulses enter the eye under a Maxwellian view with a half-opening angle of 0.4° ($d = 0.34$ mm; see Section 1), this implies that the upper limit of background photons is given by 0.074 cnt/s.

6. CONCLUSION

We have assessed the level of darkness in a dark chamber for psychophysical experiments using a single-photon avalanche photodiode. By placing the detector behind a shutter, we could compare the detector shutter-open and shutter-closed count distributions, thus providing a direct measurement of the level of darkness. From a Bayesian fit of the data taken over 616 h, we found the light level to be below 0.039 cnt/s (0.95 HDI), while the posterior distribution exhibited a probability of positive direction of 0.42 (uncertain whether an effect is present) and substantial to decisive evidence (based on the Savage–Dickey

ratio) for absolute darkness depending on the prior distribution chosen. On the other hand, we estimated a light level of $(6.9 \pm 1.8) \times 10^{-10}$ cnt/s from an environment-attenuation approach, in which the light level in the lab and the attenuation of the dark chamber were evaluated. The exact interpretation of this last number, however, is problematic. Although we have conducted this work in light of psychophysical experiments, the method is directly applicable to all experiments in which a null background is of high importance.

Funding. Nederlandse Organisatie voor Wetenschappelijk Onderzoek (024.003.037); Ministerie van Economische Zaken en Klimaat; Horizon 2020 Framework Programme (862035).

Acknowledgment. We acknowledge funding from NWO/OCW (Quantum Software Consortium), from the Dutch Ministry of Economic Affairs (Quantum Delta NL), and from the European Union's Horizon 2020 research and innovation program (QLUSTER).

Disclosures. The authors declare no conflicts of interest.

Data availability. The data underlying this paper and example evaluation scripts are available in Ref. [27].

Supplemental document. See Supplement 1 for supporting information of the methodology used.

REFERENCES

1. D. Koenig and H. Hofer, "The absolute threshold of cone vision," J. Vis. **11**(1), 21 (2011).
2. S. Hecht, S. Schlaer, and M. H. Pirenne, "Energy at the threshold of vision," Science **93**, 585–587 (1941).
3. B. Sakitt, "Counting every quantum," J. Physiol. **223**, 131–150 (1972).
4. M. C. Teich, P. R. Prucnal, G. Vannucci, *et al.*, "Multiplication noise in the human visual system at threshold: 1. Quantum fluctuations and minimum detectable energy," J. Opt. Soc. Am. **72**, 419–431 (1982).
5. J. N. Tinsley, M. I. Molodtsov, R. Prevedel, *et al.*, "Direct detection of a single photon by humans," Nat. Commun. **7**, 12172 (2016).
6. T. H. A. van der Reep, D. Molenaar, W. Löffler, *et al.*, "Quantum detector tomography applied to the human visual system: a feasibility study," J. Opt. Soc. Am. A **40**, 285–293 (2023).
7. G. D. Field, V. Uzzell, E. J. Chichilnisky, *et al.*, "Temporal resolution of single-photon responses in primate rod photoreceptors and limits imposed by cellular noise," J. Neurophysiol. **121**, 255–268 (2019).
8. G. Westheimer, "The Maxwellian view," Vision Res. **6**, 669–682 (1966).
9. C. Curcio, K. Sloan, R. Kalina, *et al.*, "Human photoreceptor topography," J. Comp. Neurol. **292**, 497–523 (1990).
10. E. J. Denton and M. H. Pirenne, "The absolute sensitivity and functional stability of the human eye," J. Physiol. **123**, 417–442 (1954).
11. P. E. Hallett, F. H. C. Marriott, and F. C. Rodger, "The relationship of visual threshold to retinal position and area," J. Physiol. **160**, 364–373 (1962).
12. R. Holmes, M. Victora, R. F. Wang, *et al.*, "Measuring temporal summation in visual detection with a single-photon source," Vision Res. **140**, 33–43 (2017).
13. A. Dey, A. J. Zele, B. Feigl, *et al.*, "Threshold vision under full-field stimulation: revisiting the minimum number of quanta necessary to evoke a visual sensation," Vision Res. **180**, 1–10 (2021).
14. E.-J. Wagenmakers, M. D. Lee, T. Lodewyckx, *et al.*, "Bayesian versus frequentist inference," in *Bayesian Evaluation of Informative Hypotheses in Psychology*, H. Hoijtink, I. Klugkist, and P. A. Boelen, eds. (Springer, 2008), pp. 181–207.
15. R Core Team, *R: A Language and Environment for Statistical Computing* (R Foundation for Statistical Computing, 2017).
16. Stan Development Team, "RStan: the R interface to Stan," (2023), R package version 2.32.5.
17. G. Cassela and R. L. Berger, *Statistical Inference*, 2nd ed. (Duxbury, 2002).
18. D. Makowski, M. S. Ben-Shachar, and D. Lüdecke, "bayestestR: describing effects and their uncertainty, existence and significance within the Bayesian framework," J. Open Source Softw. **4**, 1541 (2019).
19. J. M. Dickey, "The weighted likelihood ratio, linear hypotheses on normal location parameters," Ann. Math. Statist. **42**, 204–223 (1971).
20. C. Kooperberg, Logspline: Routines for Logspline Density Estimation (2024), R package version 2.1.21.
21. H. Jeffreys, *Theory of Probability*, 3rd ed. (Oxford University, 1961).
22. Q. F. Gronau, A. Ly, and E.-J. Wagenmakers, "Informed Bayesian *t*-tests," Am. Stat. **74**, 137–143 (2020).
23. J. N. Rouder, P. L. Speckman, D. Sun, *et al.*, "Bayesian *t*-tests for accepting and rejecting the null hypothesis," Psychon. Bull. Rev. **16**, 225–237 (2009).
24. J. Love, R. Selker, M. Marsman, *et al.*, "JASP: graphical statistical software for common statistical designs," J. Stat. Softw. **88**, 1–17 (2019).
25. I. Esmaeil Zadeh, J. Chang, J. W. N. Los, *et al.*, "Superconducting nanowire single-photon detectors: a perspective on evolution, state-of-the-art, future developments, and applications," Appl. Phys. Lett. **118**, 190502 (2021).
26. E. Lantz, J.-L. Blanchet, L. Furfaro, *et al.*, "Multi-imaging and Bayesian estimation for photon counting with EMCCDs," Mon. Not. R. Astron. Soc. **386**, 2262–2270 (2008).
27. T. van der Reep, D. Molenaar, and W. Löffler, "Data: measurement of darkness (1.0.0)," Zenodo (2024), https://doi.org/10.5281/zenodo.13951375.